Magnetospheres of Jupiter and Saturn

JAMES W. HAFFNER*
North American Rockwell Corporation, Downey, Calif.

A series of calculations has been carried out to estimate the characteristics of the magnetospheres around the planets Jupiter and Saturn. Solar wind characteristics near these planets were deduced from those near the Earth using standard hydrodynamic equations. Planetary magnetic fields were estimated from nonthermal rf emissions, which were assumed to be synchrotron radiation. (Nonthermal radiation from Saturn has not been confirmed, so only a possible upper limit was used for that planet.) Based upon energy density relationships, the calculated standoff distances are $\sim 40R_J$ and $\lesssim 50R_S$ for Jupiter and Saturn, respectively. The corresponding calculated magnetospheric tail lengths are $\sim$0.5 a.u. and $\lesssim$0.7 a.u. Jupiter's Van Allen belts are $\sim$ an order of magnitude more intense than the Earth's, while Saturn's are $\lesssim$ an order of magnitude less than the Earth's. Centrifugal flattening does not appear to be a major effect for either planet's belts.

Nomenclature

a	=	effective inner radius of Van Allen belts (planetary radii)
a.u.	=	astronomical unit ($\sim 1.5 \times 10^8$ km)
b	=	effective spatial limit of coronal heating ($\sim 10R_{sun}$)
B'	=	equatorial magnetic flux density along any given field line (gauss = 10^{-4} webers/m^2)
B_0	=	equatorial surface magnetic flux density (gauss)
e	=	charge of trapped particle (1.6×10^{-19} coulomb)
G	=	universal gravitational constant (6.673×10^{-11} newton m^2/kg^2)
h	=	distance from planetary spin axis (planetary radii)
H_0	=	equatorial surface magnetic field strength (oersted)
J	=	gyrorotation angular momentum of trapped particle
k	=	Boltzmann's constant (1.38×10^{-23} joule/°K)
L	=	McIlwain magnetic field coordinate (planetary radii)
m	=	mass of proton ($\sim 1.6 \times 10^{-27}$ kg)
M_{sun}	=	sun's mass (1.99×10^{30} kg)
N	=	relative Van Allen belt particle density (≤ 1)
P	=	solar wind particle density (m^{-3})
r	=	distance from the sun (a.u.)
R	=	distance from planetary center (planetary radii)
R_{sun}	=	sun's radius ($\sim$696,000 km)
R_E	=	Earth's radius ($\sim$6371 km)
R_J	=	Jupiter's radius ($\sim$69,000 km)
R_S	=	Saturn's radius ($\sim$57,500 km)
v	=	directed velocity of solar wind (m/sec)
$v_{\|\|}$	=	component of trapped particle's velocity parallel to magnetic field line (m/sec)
$v_\perp$	=	component of trapped particle's velocity perpendicular to magnetic field line (m/sec)
α	=	pitch angle of trapped particle
α_0	=	equatorial pitch angle of trapped particle
β	=	polytrope (ideal gas) index ($\sim\frac{5}{3}$ for hydrogen)
θ	=	polar coordinate (polar angle)
θ_L	=	limiting mirroring polar coordinate for bounce motion of trapped particle
μ_0	=	permeability of free space ($4\pi \times 10^{-7}$ h/m)
ρ	=	polar coordinate (the radius)
ω	=	angular velocity of planetary spin (rad/sec)

Introduction

JUPITER and Saturn are two of the most interesting objects in our solar system. Because of the planned unmanned spacecraft missions to these two planets, their expected environments are of renewed interest. The magnetic field parameters constitute one of these important environments.

This paper is concerned primarily with the spatial extent of the magnetospheres of the planets Jupiter and Saturn. This spatial extent is a consequence of the planetary magnetic fields, the solar wind (carrying the solar magnetic field frozen in), and the interaction between them. Fortunately, the Earth's magnetosphere provides a useful model. The Earth's magnetic field is essentially that of a dipole, possessing a field strength of $\sim$0.3 oe at the equatorial surface of the Earth. This dipole is oriented within $\lesssim 20°$ of the normal to the direction of the solar wind particles (essentially all protons and electrons). The solar wind at 1 a.u. from the sun has a velocity of 300–800 km/sec, a particle density of 0.5–30 cm^{-3}, and an effective temperature of 1–3 $\times 10^5$°K. As a result, the Earth's magnetosphere has a time-varying standoff radius of 6–15R_E, a maximum width of 20–50R_E and a tail length of 200–500R_E (Fig. 1). Within this quasi-teardrop-shaped volume, the Earth's magnetic field is dominant; outside it the solar magnetic field is dominant. Spacecraft crossing the turbulent boundary (magnetopause) experience discontinuities in magnetic field direction and charged particle flux parameters.

The magnetic field and charged particle flux parameters will change as spacecraft cross the magnetopauses of the planets Jupiter and Saturn. The spatial dimensions of these magnetopauses and the particle and field environments they contain are of direct interest. A calculation of these parameters is described in the following sections of this paper.

Solar Wind Characteristics

Direct measurements of the solar wind have been carried out only between 0.7 and 1.5 a.u. from the sun. Indirect measurements via the observation of Class I comet tails have extended this somewhat, but beyond 2 a.u. only calculations provide estimates of solar wind parameters as of now. Among the calculation assumptions, based upon direct and indirect measurements, is that the solar wind is an electrically neutral plasma obeying hydrodynamic-like equations. Thus, the solar wind expands outward from the sun as a gas through a nozzle, gaining kinetic energy at the expense of internal (thermal) energy. The expansion is not adiabatic close to the sun since the gravitational, magnetic, and radiation fields

Presented as Paper 71-30 at the AIAA 9th Aerospace Sciences Meeting, New York, January 25–27, 1971; submitted January 25, 1971; revision received July 12, 1971.

* Staff Scientist, Space Division. Associate Fellow AIAA.

of the sun perturb it. The ~27-day rotation of the sun results in spiral lines of magnetic flux even though the individual particles travel outward in essentially straight radial lines. Various types of plasma waves, as well as the high electron velocities (electron temperatures are typically 1.5–5 times proton temperatures) effectively transfer energy across the spiral lines of magnetic flux. However, since the solar wind becomes supersonic at 3–5R_{sun} plasma oscillations cannot transfer energy longitudinally. At 1 a.u. the Mach number is ~7.

The quiet day solar wind in the frame of reference rotating with the sun is generally assumed to obey Bernoulli's equation.[1-3] This equation may be written

$$\tfrac{1}{2}mv^2 - GM_{sun}m/r + \beta kT/(\beta - 1) = E \qquad (1)$$

where T is the effective plasma temperature, E is total energy of the plasma expansion, and the Nomenclature defines the other variables. β increases from slightly greater than unity near the solar corona to $\frac{5}{3}$ for adiabatic expansion.

While v and T are functions of r in the form of Bernoulli's equation given previously, the solution behavior as r becomes large is of interest here. The solutions to Bernoulli's equation fall into three general classes. For solutions of the first class, the streaming velocity approaches 0 at both $r \to 0$ and $r \to \infty$. For solutions of the second class the streaming velocity becomes large at both these spatial limits. For the third solution, the critical solution, the streaming velocity is small for small r, increasing monotonically as r increases, and approaches an asymptotic value as $r \to \infty$. As Parker has pointed out, not only is this the solution of physical interest, but it represents a stable equilibrium.

The behavior of the directed solar wind velocity as a function of distance from the sun has been calculated by several researchers. There are some differences based upon the near-sun temperature, density, and particle mass distributions, but the gross behavior is that shown in Fig. 2. The range of values measured in the vicinity of 1 a.u. is 300–800 km/sec. Thus, the average calculated value of 350 km/sec at 1 a.u. agrees well with the measurements. As r becomes large, the mathematical behavior of the directed (streaming) velocity is expected to asymptotically approach ~400 km/sec. This may be seen from the asymptotic behavior of the critical energy solution

$$\lim[\tfrac{1}{2}mv^2] \to 2kT_0 \ln(r/r_0) + GM_{sun}m/r - \tfrac{3}{2}kT_0 + \ldots \qquad (2)$$

where r_0 is the critical radius, which lies at ~10R_{sun}, and T_0 is the effective solar wind temperature at this distance ($T_0 \sim 10^6$°K). As $r \to \infty$,

$$[\tfrac{1}{2}mv^2] \to 2kT_0 \ln(b/r_0 + 1) \qquad (3)$$

which is a constant (~1.3×10^{-9} ergs/particle) yielding ~400 km/sec.

The temperature dependence of the solar wind as a function of distance from the sun, based upon Bernoulli's equation, obeys the relationship

$$[v(r)/v(b)]^2 = (b/r)^4[T(b)/T(r)]^3 \qquad (4)$$

Thus, so long as the directed velocity is increasing the effective temperature decreases nonadiabatically even though the effects of energy input and gravitational attraction are negligible. However, after the directed velocity has become essentially constant, the effective temperature decreases as $r^{-4/3}$ (i.e., adiabatically).

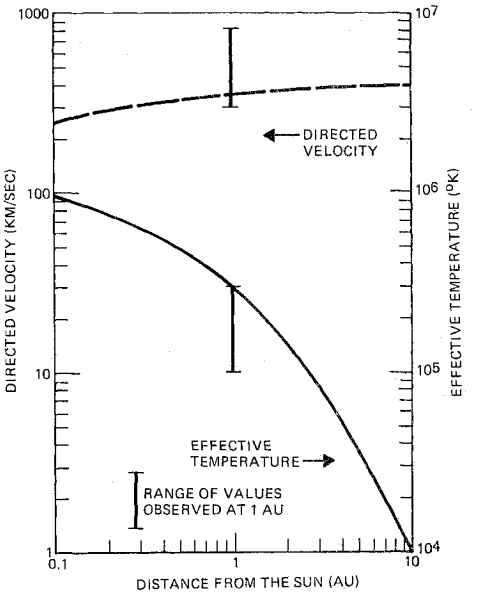

Fig. 2 Directed velocity and effective temperature of the solar wind as functions of distance from the sun.

The calculated quiet sun effective temperature of the solar wind as a function of distance from the sun is also shown in Fig. 2. The behavior out to ~10R_{sun} is based upon published calculations of other researchers.[1,4] The range of values observed in the vicinity of 1 a.u. is also shown. Agreement with calculations is good. It should be pointed out that the effective temperature is due primarily to the protons. The electron temperatures have relatively little effect on the effective solar wind temperature, as the mass of the protons and the electron-proton coulomb attraction result in the electrons' following wherever the protons go.

The particle flux of the solar wind protons and electrons must fall off as r^{-2}, unless some mechanism prevents the solar wind from being isotropically emitted from the sun. In the absence of data outside the ecliptic plane, it is assumed that no external environment acts to limit the polar solar wind. The solar temperature (and presumably the solar wind emission) is essentially uniform as a function of latitude, even though solar activity is observed primarily at ±5° → 35° solar latitude. The only known difference between solar polar and equatorial conditions is solar rotation and its resultant centrifugal force. However, this centrifugal force is small compared with gravitational attraction or coronal temperature expansion forces. Consequently, an inverse square particle density is assumed, normalized to 5 cm^{-3} at 1 a.u. (observed values range from 0.5–30 cm^{-3}).

One significant effect of solar rotation, however, is on the shape of the solar magnetic field which the solar wind carries frozen in. In contrast to the individual particles (which stream radially outward from sun) the magnetic field lines connect particles emitted from the same solar region. Consequently, the magnetic field lines are spirals making an angle of ~45° at 1 a.u. with the radial. Beyond 1 a.u. the solar wind velocity is almost constant, so the cumulative angle increases ~58° every a.u. thereafter. Thus, the solar magnetic field cumulative angle will be 290° at the orbit of Jupiter (5.2 a.u.) and ~540° at the orbit of Saturn (9.5 a.u.). The hose angle (angle between the direction of proton travel and the solar magnetic field) at Jupiter is thus ~78° and ~83° at Saturn (Fig. 3).

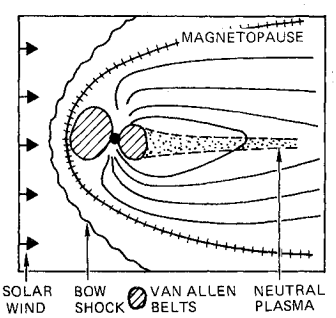

Fig. 1 Geometry of the Earth's magnetosphere in the plane of the solar wind.

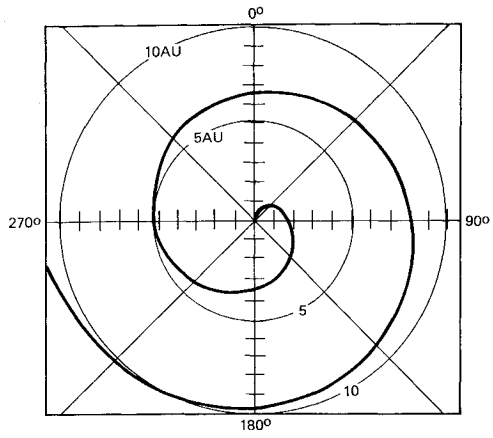

Fig. 3 Direction of solar magnetic field as a function of distance from the sun.

Based upon the preceding, it is possible to make quantitative estimates of the solar wind properties at Jupiter and Saturn. The results are given in Table 1.

The flux and velocity values for 5.2 a.u. agree fairly well with those calculated by Scarf.[5] His effective temperatures are lower, even at 1 a.u. The range of Vela measurements makes selection of an effective temperature difficult, but the higher values appear more often.

Some remarks concerning the probable validity of these solar wind parameters are in order. For these numbers to be valid, the heliosphere must lie appreciably beyond 9.5 a.u. E. N. Parker,[1] J. B. Weddell,[6] and others have carried out calculations concerning the size of the heliosphere. Values from 2 a.u. to 100 a.u. have been reported. It is generally agreed that Jupiter has Van Allen belts, and thus lies within the heliosphere since the solar wind is almost certainly the major source of Van Allen belt particles. Saturn may have Van Allen belts, and thus the heliosphere may lie beyond 9.5 a.u. (The uncertainty of Saturn's 10-cm polarization measurements could conceivably be due to Saturn's crossing the heliospheric boundary.) One simple way to estimate the heliospheric radius is based on the energy density of the galactic magnetic field. Galactic protons with energies approaching 10^{19} ev have been observed (via air showers) at 1 a.u. Our galaxy is $\sim 10^5$ light years ($\sim 10^{23}$ cm) across. Since the energy density of galactic particles at 1 a.u. is approximately that of starlight at 1 a.u. ($\sim$1 ev/cm^3, excluding light from our sun) the galactic particles are believed to be trapped (up to $\sim 10^{19}$ ev). To trap a 10^{19} ev proton in a cavity 10^{23} cm across requires a spatially averaged magnetic field of $\sim$1 gamma (which agrees with estimates based on galactic radio noise—assumed to be synchrotron emission—and the Zeeman splitting of the 21 cm hydrogen line). A 1 gamma field represents an energy density of $\sim$2.5 ev/cm^3. At 1 a.u. the solar wind has an energy density of $\sim$3 kev/cm^3. Based upon an inverse square spatial relationship, the solar wind energy density will approach 2.5 ev/cm^3 at $\sim$35 a.u., which is one estimate of the heliospheric standoff radius.

Scarf[5] has considered various types of plasma oscillations which might lead to instability, thus invalidating the assumptions of isentropic expansion and inverse square density behavior. He concludes that whereas whistler oscillations will arise when the electron temperature has dropped to the point that they are supersonic (protons become supersonic at $\sim 5R_{sun}$), the time averaged solar wind properties can be calculated using these assumptions.

Planetary Magnetic Fields

In the absence of direct measurements of the magnetic fields of Jupiter and Saturn, it is necessary to use indirect means to estimate them. The indirect information available consists of rf radiations emitted by these planets and received at the Earth. These rf radiations yield an effective black-body temperature which is an increasing function of wavelength for wavelengths of 1–100 cm.[7] Whereas part of this effect may be due to the temperature profiles of the planets' atmospheres[8] (the longer the wavelength, the deeper in the atmosphere its effective source lies), for Jupiter part of this effect is almost certainly due to synchrotron emission from that planet's Van Allen belt electrons.[9] The evidence for that planet is convincing. The spatial distribution of the decimetric emissions has been measured, showing that it lies beyond the planet itself. Decametric bursts have been observed whose emission probability correlates well with the position of Jupiter's first large moon, Io. Both decimetric and decametric rf noises exhibit polarizations—linear for the decimeter noise, and elliptical for the decameter bursts (but most of this may be due to the Earth's ionosphere). If these radiations were thermal in origin they would be unpolarized. For Saturn, only upper limits can be set for the nonthermal rf radiations observed at the Earth.[10] Less than 10% of the decimeter radiation comes from outside the planetary disk, and less than 6% of the decimetric radiation is linearly polarized. However, decametric bursts (unconfirmed) have been observed attributed to Saturn,[11] and that planet's rapid rotation strongly suggests a sizable dipole magnetic field. Based upon this evidence, for the purposes of these calculations it has been assumed that both Jupiter and Saturn have dipole magnetic fields.

The basic logic for determining the strength of these magnetic fields is straightforward. It is assumed that the total nonthermal decimetric radiation can be obtained by an isotropic integration over a sphere centered in the planet and containing the Earth on its surface. It is further assumed that this nonthermal decimetric radiation is synchrotron radiation from relativistic electrons trapped in a dipole magnetic field. A characteristic of synchrotron emission is that the power radiated per electron increases essentially linearly with the strength of the ambient magnetic field. Consequently, the stronger the planetary magnetic field, the fewer the necessary electrons to account for the observed decimetric radiation. Alternatively, the weaker the planetary magnetic field strength, the more electrons which are required. However, there is a maximum number of electrons which can be stably trapped by a given magnetic field configuration.[12] The weaker the planetary magnetic field, the fewer the electrons which can be trapped. For each planet there exists a minimum magnetic field strength which can barely hold enough electrons to account for the radiated decimetric power. In a previous paper[13] this logic was applied to the planet Jupiter, yielding the relationship

$$H_0 \geq 0.44 a^{2.29} N^{-0.236} \text{ oe} \qquad (5)$$

where a is in Jupiter radii and $N = 1$ for saturated belts. Using the Earth's belts as a model, N is $\sim 3 \times 10^{-3}$ (N is $\sim 10^{-1}$ for the Earth, time averaged). While a for the Earth is $\sim 1.2\ R_E$, Jupiter at one time was believed to have a highly eccentric magnetic field, which would act to increase a. However, it is improbable that a body as large and rapidly

Table 1 Calculated solar wind properties at Jupiter and Saturn

	Earth (1 a.u.)	Jupiter (5.2 a.u.)	Saturn (9.5 a.u.)
Particle density	5 cm^{-3}	0.2 cm^{-3}	0.06 cm^{-3}
Directed velocity	350 km/sec	400 km/sec	400 km/sec
Effective temperature	3×10^5°K	3.3×10^4°K	1.5×10^4°K
Mach number	7	23	35

rotating as Jupiter, especially considering its low average density, has its ferromagnetic materials (responsible for its magnetic field) appreciably off center.[7] Consequently, a value of $\sim 1.3R_J$ was chosen for the parameter a. These values of N and a yield $H_0 \sim 3$ oe ($B_0 \sim 3$ gauss) at Jupiter's visible equator. This value is somewhat less than the 10–15 gauss usually quoted, but the disagreement is not serious considering that most estimates (including this one) are probably ± a factor of 3.

A similar analysis[10] has been carried out for the planet Saturn, based upon a nonthermal decimetric flux at the Earth of 5×10^{-18} w/m^2 (5% of the rf emitted for $\lambda \geq 5$ cm). This integrates to a radiated power of 5×10^6 watts, as compared with Jupiter's nonthermal emission of 2.7×10^9 w. The remainder of the calculation proceeds as for Jupiter, leading to the relationship

$$H_0 \geq 0.11a^{2.29}N^{-0.236} \text{ oe} \tag{6}$$

However, the rings of Saturn constrain a to values $>2.3R_S$, probably even $>2.44R_S$ (Roche's limit). The low solar wind flux (the most probable source of the Earth's Van Allen belt particles, and possibly Saturn's as well) acts to limit N to $\sim 10^{-3}$. Thus, for Saturn H_0 is probably ~ 3 oe ± a factor of 3, the same value calculated for Jupiter. However, since Jupiter is ~20% larger in linear dimensions than Saturn, its dipole moment will be ~44% larger than Saturn's due to this effect alone.

It should be pointed out that for both Jupiter and Saturn it has been assumed that the magnetic dipole is essentially parallel to the spin axis. Jupiter's magnetic dipole is within 10° of its spin axis, based upon the rocking of the decimetric linear plane of polarization. According to Zheleznyakov[14] and Zlotnik[15] the plane of polarization for Saturn's possibly nonthermal decimetric radiation lies parallel to its spin axis, while Jupiter's plane of polarization is essentially parallel to its equator. However, this is believed to be due to the electron equatorial pitch angle distribution. For Jupiter this pitch angle distribution peaks near 90°, which means many of the electrons spend much of their time near the magnetic equator, whereas for Saturn the distribution peaks near 0°, which means that the electrons spend much of their time near the poles. This may be due to Saturn's rings, since an electron with a small equatorial pitch angle has a better chance of traversing the ring plane without colliding with a ring particle.

Magnetospheric Dimensions

The magnetosphere of a planet with a dipole field (e.g., the Earth) is a teardrop-shaped volume with the tail pointing in the antisolar direction. For the Earth (equatorial surface magnetic field strength ~0.3 oe) the magnetosphere has a standoff radius of $\sim 10R_E$ in the solar direction, ~30 R_E radius at its widest point, and a tail length of ~200–500 R_E. It is possible to calculate these numbers from simple physical considerations.

The sunward standoff radius may be calculated by equating the energy densities of the planetary magnetic field and of the solar wind.[1,16] The relationship

$$B_0^2/(2\mu_0 R^6) = \tfrac{1}{2}Pmv^2 \tag{7}$$

yields

$$R = (B_0/v)^{1/3}(1/\mu_0 Pm)^{1/6} \tag{8}$$

where r is in planetary radii. Substituting mks values for the Earth yields $\sim 10R_E$, in good agreement with the time averaged quiet sun value. Applying similar logic for Jupiter and Saturn yields (based upon $B_0 = 3$ gauss and $v = 400$ km/sec) for Jupiter

$$r = 40R_J(P \sim 2 \times 10^5 m^{-3})$$

Table 2 Calculated peak Van Allen belt particle flux rates

	Jupiter	Saturn
$\hat{\phi}_e > E$ electrons/(cm^2-sec)	$1.6 \times 10^9 e^{-E/E_0}$	$4.3 \times 10^7 e^{-E/E_0}$
$\hat{\phi}_p > E$ protons/(cm^2-sec)	$5.7 \times 10^7 e^{-E/E_0'}$	$1.5 \times 10^5 e^{-E/E_0'}$

and for Saturn

$$r = 50R_S(P \sim 6 \times 10^4 m^{-3})$$

It will be seen that these values are relatively insensitive to the input variables. Thus, even though B_0 has uncertainties of ± a factor of 3 and P has uncertainties of perhaps as much as a factor of 2, these standoff radii are probably correct to ±50%.

The length of the Earth's magnetospheric tail[17] may be calculated by multiplying the maximum width of the magnetosphere (~3 × the standoff radius) by the local solar wind Mach number. For the Earth the quiet sun Mach number is ~7 (directed velocity ~350 km/sec, thermal velocity or ~50 km/sec, based on an effective temperature of 3×10^5°K). This leads to a tail length of $10R_E \times 3 \times 7 = \sim 210R_E$. The total length of the Earth's magnetospheric cavity is thus $250R_E$ ($\sim 10R_E$ standoff + $\sim 30R_E$ to the maximum cavity width + $\sim 210R_E$ tail length). Applying similar logic to Jupiter and Saturn yields magnetospheric tail lengths of $\sim 1000R_J$ and $\sim 1700R_S$, respectively. The maximum magnetospheric cavity widths are 1.7×10^7 km for both planets ($R_J \sim 6.9 \times 10^4$ km, $R_S \sim 5.75 \times 10^4$ km). The total calculated lengths of the magnetospheric cavities are ~0.5 a.u. and ~0.7 a.u. for Jupiter and Saturn, respectively. Thus, all of their respective natural satellites spend time inside the magnetospheres, and many of them are never exposed to the solar wind at all.

Inside these enormous magnetospheres, Jupiter and Saturn have Van Allen belts. The plasma stability limited fluxes vary as (L^{-4}).[12] The general formulas developed in a previous publication for these trapped electron and proton fluxes are[13]

$$\phi_e(>E) = 3.5 \times 10^{11} NL^{-4}H_0^{4/3}e^{-E/E_0} \text{ electrons/cm}^2\text{-sec} \tag{9}$$

where

$$E_0 = 5.25H_0^{0.455}L^{-1.36}\text{Mev}$$

$$\phi_p(>E) = 1.25 \times 10^9 NL^{-4}H_0^{4/3}e^{-E/E_0'} \text{ protons/cm}^2\text{-sec} \tag{10}$$

where

$$E_0' = 3000H_0^{5/3}L^{-5}\text{Mev}$$

Substituting values calculated earlier ($H_0 = 3$ oe, $N_J \sim 3 \times 10^{-3}$, $N_S \sim 10^{-3}$, $L_{\min} \equiv a = 1.3R_J$ for Jupiter, $2.44R_S$ for Saturn) leads to the peak flux rates listed in Table 2. Thus, Jupiter's calculated equatorial peak fluxes are an order of magnitude larger than those of the Earth, while Saturn's are an order of magnitude smaller. These numbers are quite dependent upon the choice of H_0, N and a, and have associated uncertainties of ± an order of magnitude.

Because of the large sizes and rapid rotations of Jupiter and Saturn, the effects of centrifugal force are approximately 25 times more important than on corresponding L shells at the Earth. However, while centrifugal forces exceed gravitational forces beyond $\sim 2.3R_J$ and $\sim 1.9R_S$ for Jupiter and Saturn, respectively, both are relatively unimportant compared with magnetic forces. It has been customary to treat the Van Allen belts as a plasma for many purposes (especially the analysis of transient disturbances). However, the influence of the planetary magnetic field on each trapped par-

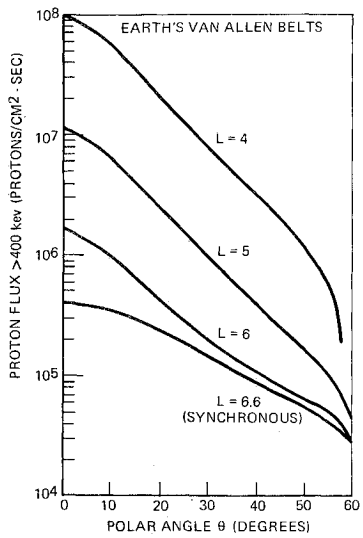

Fig. 4 Distribution of low energy proton flux along magnetic flux lines in Earth's Van Allen belts.

ticle must be greater than that of the other charged particles—this is the condition necessary for stable trapping. The Van Allen belts are not a plasma in the sense that each charged particle is primarily influenced by all the other particles in the plasma.

The trapped particle flux distributions along lines of magnetic flux are a function of the L value in the Earth's Van Allen belts (see Fig. 4). As synchronous orbit (6.6 R_E) is approached, the distribution becomes more uniform as a function of the polar angle θ. For Jupiter synchronous orbit is at $2.3R_J$ while for Saturn it is at $1.9R_S$ which means most of Jupiter's Van Allen belts and all of Saturn's Van Allen belts lie beyond synchronous orbit. Consequently, a fairly uniform particle flux distribution is expected as a function of θ.

It is possible to quantitatively evaluate the influence of planetary rotation on the spatial distribution. The "bouncing" of the trapped particles between its mirror points is analogous to a bead sliding on a frictionless wire bent in the shape of a magnetic line of force. For a dipole field these lines of force have a shape given by the equation

$$\rho = L \sin^2\theta \tag{11}$$

The lines of magnetic flux, having no mass, are not perturbed by planetary rotation except possibly near the magnetopause. If there is no centrifugal force due to planetary rotation, the trapped particle's total velocity is a constant of the motion (a time independent magnetic field cannot exchange energy with a charged particle). Thus

$$B/\sin^2\alpha = m^2v^2/(Je) = \text{constant} \tag{12}$$

where the trapped particle spirals around the magnetic line of flux. For a dipole field

$$B = B_0\rho^{-3}(3\cos^2\theta + 1)^{1/2} = B_0L^{-3}\sin^{-6}\theta(3\cos^2\theta + 1)^{1/2} \tag{13}$$

Thus, the trapped particle will mirror at the limiting polar angle θ_L given by the equation

$$B/B' = (3\cos^2\theta + 1)^{1/2}/\sin^6\theta = \sin^{-2}\alpha_0 \tag{14}$$

where B' is taken along the field line about which the trapped particle is spiraling. Considering the velocity component of the trapped particle parallel to the magnetic field line ($v_{||}$), it can be shown that

$$\begin{aligned} v_{||} &= v^2 - JeB/m^2 \\ &= v^2 - JeB'(3\cos^2\theta + 1)^{1/2}/(m^2\sin^6\theta) \end{aligned} \tag{15}$$

The mirror points occur at those values of θ for which $v_{||}$ vanishes. Physically the particle exchanges bounce kinetic energy (represented by $v_{||}^2$) for potential energy (represented by JeB/m) as it goes from the magnetic equator to the mirror point.

If planetary rotation is now introduced, the centrifugal potential represents another energy storage mechanism which $v_{||}$ must satisfy as θ increases. The equation becomes

$$\begin{aligned} v_{||} &= v^2 - JeB'(3\cos^2\theta + 1)^{1/2}/(m^2\sin^6\theta) - \omega^2h^2 \\ &= v^2 - JeB_0(3\cos^2\theta + 1)^{1/2}/(m^2L^3\sin^6\theta) - \\ &\qquad \omega^2L^2\sin^6\theta \end{aligned} \tag{16}$$

where h is taken to the magnetic line of flux the trapped particle is spiralling about. Again, the mirror point is that at which $v_{||}$ vanishes. This will occur at a smaller value of θ because of planetary rotation than was the case when ω (the planetary angular velocity) was zero. The extent of this effect on θ_L indicates the amount of centrifugal flattening to be expected, assuming that the source and loss mechanisms (which will produce an equilibrium equatorial pitch angle distribution in the absence of planetary rotation) are not otherwise affected.

For particles trapped in Jupiter's magnetic field, the equation simplifies to

$$v_{||}^2 = v^2(1 - \sin^2\alpha) - 1.47 \times 10^8L^2\sin^6\theta \tag{17}$$

where v is the particle velocity (m/sec), and L is in Jupiter radii. For the centrifugal term to be comparable to the magnetic term (represented by $v^2\sin^2\alpha$), v must be comparable to 1.2×10^4L. This condition occurs for low energy protons ($E \lesssim 1$ kev) at large L values ($L \gtrsim 30$). Since the characteristic proton energy (E_0) is $\sim$1 kev at the outer edge of the Jovian Van Allen belt, these particles will mirror at $\theta_L \sim 30°$ (as contrasted to $\theta_L \sim 70°$ had the centrifugal effect been absent. However, for $E \gtrsim 10$ kev, the reduction in θ_L is $\lesssim 1°$ (Fig. 5). Consequently, while some flattening of Jupiter's Van Allen belts is expected due to centrifugal force, this is not expected to be a major effect. For Saturn the effect will be less because the planet is $\sim$20% smaller and rotates $\sim$6% less rapidly.

Conclusions

Calculations show that the solar wind expands essentially isentropically beyond 1 a.u. at a directed velocity of $\sim$400 km/sec. Its particle density ($\sim$5 cm^{-3} at 1 a.u.) obeys an

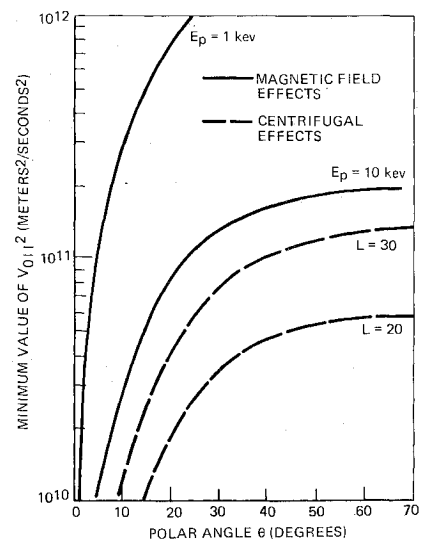

Fig. 5 $V_{0||}$, required due to magnetic field effect and centrifugal force effect for Jupiter's Van Allen belt (B_0 = 3 gauss).

inverse square distance relationship. It most probably continues past the orbit of Saturn (9.5 a.u.). Based upon an analysis of rf noise from the planets Jupiter and Saturn, both have surface equatorial magnetic fields of 3 gauss ± a factor of 3 (assumed to be dipoles). These magnetic fields produce teardrop-shaped cavities (magnetospheres) in the solar wind with standoff radii of $\sim 40 R_J$ and $\lesssim 50 R_S$ at Jupiter and Saturn, respectively. Magnetospheric cavity widths of $\sim 1.7 \times 10^7$ km (each planet) and tail lengths of ~ 0.5 a.u. (Jupiter) and $\lesssim 0.7$ a.u. (Saturn) were calculated based upon effective solar wind temperatures of 3.3×10^4°K (5.2 a.u.) and 1.5×10^4°K (9.5 a.u.). Jupiter's calculated Van Allen belts have time averaged peak fluxes ($\sim 10^9$ e/cm^2-sec) an order of magnitude above those of the Earth, while Saturn's belt fluxes ($\lesssim 10^7$ e/cm^2-sec) are an order of magnitude less than Earth's. The centrifugal effects of planetary rotation will flatten the particle distributions along the magnetic field lines only for low energy particles in the outer portions of the Van Allen belts.

References

[1] Parker, E. N., *Interplanetary Dynamical Processes*, Interscience, New York, 1963, Chap. 5, pp. 51–72.

[2] Scarf, F. L., "The Solar Wind and Its Interaction with Magnetic Fields," *Space Physics*, edited by D. P. LeGalley and A. Rosen, Wiley, New York, 1964, pp. 437–473.

[3] Williams, D. J. and Mead, G. D., eds., *Magnetospheric Physics*, American Geophysical Union, Washington, D.C., 1969, pp. 1–96.

[4] Bernstein, W., "The Solar Plasma—Its Detection, Measurement, and Significance," *Space Physics*, edited by D. P. LeGalley and A. Rosen, Wiley, New York, 1964, Chap. 11, pp. 397–436.

[5] Scarf, F. L., "Characteristics of the Solar Wind Near the Orbit of Jupiter," *Planetary and Space Sciences*, Vol. 17, 1969, pp. 595–608.

[6] Weddell, J. B., "Heliosphere Radius and Pressure Equilibrium Conditions," SD 70-367, 1970, North American Rockwell Corp., Downey, Calif.

[7] Newburn, R. L., Jr. and Gulkis, S., "A Brief Survey of the Outer Planets Jupiter, Saturn, Uranus, Neptune, Pluto, and Their Satellites," 32-1529, April 1971, Jet Propulsion Lab., Pasadena, Calif.

[8] Gulkis, S., McDonough, T. R., and Craft, H., "The Microwave Spectrum of Saturn," *Icarus*, Vol. 10, 1969, pp. 421–427.

[9] Michaux, C. M., *Handbook of the Physical Properties of the Planet Jupiter*, NASA SP-3031, 1967, pp. 47–62.

[10] Haffner, J. W., "The Calculated Environment of the Planet Saturn," SD 70-561, 1970, North American Rockwell Corp., Downey, Calif.

[11] Smith, A. G. et al., "Decameter Wavelength Observations of Jupiter—The Apparitions of 1961 and 1962," *Astrophysical Journal*, Vol. 141, Feb. 1965, pp. 457–477.

[12] Kennell, C. F. and Petscheck, H. E., "Limit on Stably Trapped Particle Fluxes," *Journal of Geophysical Research*, Vol. 71, No. 1, 1966, pp. 1–28.

[13] Haffner, J. W., "Calculated Dose Rates in Jupiter's Van Allen Belts," *AIAA Journal*, Vol. 7, No. 12, Dec. 1969, pp. 2305–2311.

[14] Zheleznyakov, V. V., "On the Configuration of the Magnetic Field of Saturn," *Soviet Astronomy*, Vol. 8, March–April, 1965, pp. 765–770.

[15] Zlotnik, E. Y., "The Influence of Saturn's Rings on Its Exosphere and Magnetic Field," *Soviet Astronomy*, Vol. 11, Nov.–Dec. 1967, pp. 462–470.

[16] Carr, T. D. and Gulkis, S., "The Magnetosphere of Jupiter," *Annual Review of Astronomy & Astrophysics*, Vol. 7, 1969, pp. 577–618.

[17] Ness, N. F., "The Geomagnetic Tail," *Magnetospheric Physics*, edited by D. J. Williams and G. D. Mead, American Geophysical Union, Washington, D.C., 1969, pp. 97–127.